

Using operator covariance to disentangle scaling dimensions in lattice models

Anders W. Sandvik*

Department of Physics, Boston University, 590 Commonwealth Avenue, Boston, Massachusetts 02215

(Dated: June 19, 2024)

In critical lattice models, distance (r) dependent correlation functions contain power laws $r^{-2\Delta}$ governed by scaling dimensions Δ of an underlying continuum field theory. In Monte Carlo simulations and other numerical approaches, the leading dimensions can be extracted by data fitting, which can be difficult when two or more powers contribute significantly. Here a method utilizing covariance between multiple lattice operators is developed where the r dependent eigenvalues of the covariance matrix represent scaling dimensions of individual field operators. The scheme is tested on symmetric operators in the two-dimensional tricritical Blume-Capel model, where the two relevant dimensions, as well as some irrelevant ones, are isolated along with their corresponding eigenvectors. The method will be broadly useful in studies of classical and quantum models at multicritical points and for targeting irrelevant operators at simple critical (or multicritical) points.

The most direct bridge between a critical point in a lattice model and its continuum field theoretical description is through the spectrum of scaling dimensions Δ_i . In numerical studies, e.g., Monte Carlo (MC) simulations, the dimensions are accessible in correlation functions, which contain contributions decaying with distance r as $r^{-2\Delta_i}$ for each field operator i compatible with the symmetries of the lattice operator used. For a system in d dimensions (space-time dimensions of a quantum system) the scaling dimensions of relevant operators ($\Delta_i < d$) in different symmetry sectors are related to the conventional critical exponents. While these relevant scaling dimensions are often of primary interest, irrelevant operators ($\Delta_i > d$) can produce significant corrections that complicate the analysis. To more completely characterize a critical point, determining some of the irrelevant scaling dimension is useful in its own right. Modern conformal field theory (CFT) techniques, the numerical bootstrap [1] and fuzzy sphere [2, 3], in particular, can access an extended range of scaling dimensions. In comparative studies it is then desirable to extract both relevant and irrelevant dimensions also in lattice simulations.

Operator covariance.—Here a method of disentangling different power-law contributions to lattice correlators is proposed. Defining a set of a small number of lattice operators $O_i(\mathbf{x})$, $i = 1, \dots, n$ (with $n < 10$ typically) on cells centered on position \mathbf{x} , the full covariance matrix of these operators

$$C_{ij}(\mathbf{r}) = \langle O_i(\mathbf{x}_1)O_j(\mathbf{x}_2) \rangle - \langle O_i \rangle \langle O_j \rangle, \quad \mathbf{r} = \mathbf{x}_2 - \mathbf{x}_1, \quad (1)$$

is evaluated versus the separation \mathbf{r} . The expectation value also involves averaging over equivalent pairs of lattice sites ($\mathbf{x}_1, \mathbf{x}_2$) (and $\langle O_i \rangle$ is also a spatial average). The setup is schematically illustrated in Fig. 1(a), with Fig. 1(b) depicting operators on 2×2 lattice plaquettes in the two-dimensional (2D) Blume-Capel (BC) model that will be studied here as an example.

Diagonalizing the symmetric matrix $C(\mathbf{r})$ by an orthogonal transformation $U(\mathbf{r})$,

$$D(\mathbf{r}) = U^T(\mathbf{r})C(\mathbf{r})U(\mathbf{r}), \quad (2)$$

the eigenvalues $D_i(\mathbf{r}) \equiv D_{ii}(\mathbf{r})$ represent the correlation functions of orthogonal operators Q_i . The original operators can be arranged as a columnar vector O , so that $C(\mathbf{r}) = \langle O(\mathbf{x}_1)O^T(\mathbf{x}_2) \rangle$, and, for given \mathbf{r} , the eigenoperators are the elements of $Q(\mathbf{x}) = U^T(\mathbf{r})O(\mathbf{x})$. The claim made here is that the r dependence of $D_i(\mathbf{r})$ at a critical point is predominantly of the form $D_i(r) \sim r^{-2\Delta_i}$, with Δ_i , $i = 1, \dots, n$, being scaling dimensions of the underlying CFT (or possibly other field theory) in the symmetry sector of the operators used. The validity of this claim will be confirmed with the example of the BC model at its tricritical point.

In a system described by a CFT, the method should be expected to work on account of the fact that a given lattice operator can be expanded as a sum over orthogonal field operators whose correlation functions have no cross terms. It is in general not possible to *uniquely* define a lattice operator that contains a single field operator—explicit translations from the lattice to the field operators are only known in special cases [4, 5]—and typical lattice

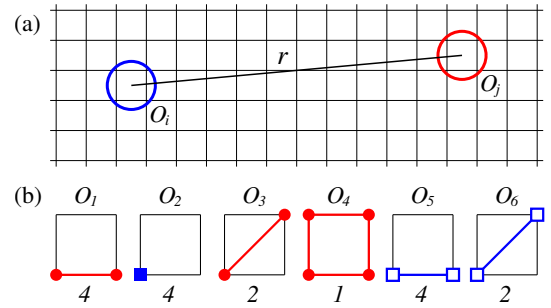


FIG. 1. (a) Operators O_i , $i = 1, \dots, n$, are defined using the degrees of freedom on multiple lattice sites and their correlation functions $C_{ij}(r)$ (the covariance matrix) are evaluated at different distances r . (b) The operators on 2×2 plaquettes used here with the 2D BC model. Red circles represent spin operators $\sigma_i \in \{-1, 0, +1\}$, blue solid squares $\sigma_i^2 \in \{0, 1\}$, open blue squares $1 - \sigma_i^2$, and colored lines imply products. The number of symmetry operations summed over are indicated beneath each plaquette.

operators contain all the symmetry-compatible CFT operators. The fact that the expansion coefficients depend on the details of the n lattice operators implies that optimal linear combinations can be found that approximate n of the orthogonal field operator. In practice, these approximants will typically represent the smallest scaling dimensions, which for sufficiently large r dominate the covariance matrix. Remaining contributions from field operators with large scaling dimensions are then negligible. The results presented below show that more scaling dimensions can be reliably extracted than what is possible by fitting conventional correlation functions.

Blume-Capel model and CFT description.—As a non-trivial example, the 2D BC model at its tricritical Ising point will be studied. The model has a three-state degree of freedom $\sigma_i \in \{-1, 0, +1\}$ on each site i of the square lattice and the Hamiltonian is

$$H = - \sum_{\langle ij \rangle} \sigma_i \sigma_j + \lambda \sum_i \sigma_i^2 \equiv E + \lambda N. \quad (3)$$

For positive $\lambda \lesssim 1.966$, the model undergoes a continuous Ising transition into a ferromagnetic state, with the critical temperature T_c decreasing as λ is increased, while for larger $\lambda \leq 2$ the transition is first-order. The location of the tricritical point (λ_t, T_t) separating these behaviors has been estimated in several works [6–13], with the most precise reported parameters being $\lambda_t \approx 1.965815$, $T_t \approx 0.608578$ from transfer-matrix calculations [10]. This point belongs to the tricritical Ising universality class, having two relevant symmetric perturbations (operators) whose scaling dimensions are $\Delta_1 = 1/5$ and $\Delta_2 = 6/5$ [5, 14]. Reproducing these values will be important but, as it turns out, several irrelevant dimensions can also be identified. Moreover, the method produces the linear combinations of the two operators E and N , defined in Eq. (3), corresponding to the relevant CFT operators. One of these eigenvectors gives the tangent of the phase boundary at the tricritical point.

Fig. 1(b) illustrates the six operators whose covariance matrix will be computed by MC simulations. Here O_1 , O_2 , and O_3 consist of terms $\sigma_i \sigma_j$ and σ_i^2 , symmetrically summed over the plaquette, O_4 is the product $\sigma_i \sigma_j \sigma_k \sigma_l$ over all four sites, and O_5 , O_6 are based on symmetrized products $(1 - \sigma_i^2)(1 - \sigma_j^2)$. The operators are normalized by the number of terms used to symmetrize, indicated in Fig. 1(b), so that their maximum value is unity.

These are not all fully symmetric operators that can be defined on 2×2 plaquettes (and larger plaquettes could also be considered) but they are sufficient, as will be demonstrated, to accurately extract several scaling dimensions. Using the procedures outlined above, the six r dependent eigenvalues $D_i(r)$ of $C(r)$ should decay as power laws $r^{-2\Delta_i}$ with, presumably, the six smallest dimensions Δ_i of fully symmetric (under spin inversion, rotations, and reflections of the 2×2 cells) operators in the tricritical Ising universality class.

For 2D CFTs with central charge $c \leq 1$, the possible values of c are $c = 1 - 6/[m(m+1)]$ for integer $m \geq 3$. The case $m = 3$ ($c = 1/2$) corresponds to the conventional Ising critical point while $m = 4$ ($c = 7/10$) is the tricritical Ising class of interest here. The primary scaling dimensions take the form

$$\Delta_{kl} = \frac{[k + m(k-l)]^2 - 1}{2m(m+1)}, \quad 1 \leq k \leq l < m. \quad (4)$$

For $m = 4$, the values corresponding to the symmetric operators studied here are $\Delta_1 \equiv \Delta_{33} = 1/5$, $\Delta_2 \equiv \Delta_{32} = 6/5$, and $\Delta_3 \equiv \Delta_{31} = 3$ ($2h_\epsilon$, $2h_{\epsilon'}$, and $2h_{\epsilon''}$ in the notation of Ref. 5). In addition to these two relevant and one irrelevant primaries, the matrix elements $C_{ij}(\mathbf{r})$ should also contain contributions from descendants, whose scaling dimensions are of the form $\Delta_i + a$ with integer $a \geq 1$. Because the operators considered are even with respect to lattice rotations (i.e., they have spin 0 in common CFT language [5]), only even- a descendants should be expected. Since Δ_1 and Δ_2 differ exactly by 1, one should expect terms $\propto r^{-2\Delta}$ with Δ taking all the values $1/5 + b$ for $b = 0, 1, 2, \dots$, as well as $3 + b$ with $b = 0$ or even valued. The amplitude of each term depends on the particular lattice operators O_i and O_j , which is at the heart of the disentangling method proposed here.

Results.—Standard MC simulations on $L \times L$ periodic lattices were carried out, combining Swendsen-Wang cluster updates [15] for the $|\sigma_i| = 1$ spins with Metropolis updates to change the number N of spins $|\sigma_i| = 1$ and to interchange $\sigma_i = 0$ and $|\sigma_j| = 1$ at different locations i, j . The model parameters $(\lambda_t, T_t) = (1.965815, 0.60858)$ from transfer-matrix calculations [10] was used for the results presented here, but nearby points were also studied, including $(1.9660, 0.6080)$ from Wang-Landau MC simulations [13]. While there are some minor differences in the results for λ and T varying within the window of uncertainty of the tricritical point, the decay exponents and eigenvectors are stable for the system sizes considered here, mainly $L = 256$. The covariance matrix was averaged over the lattice directions $(r, 0)$ and $(0, r)$.

Even though the covariance matrices of six operators were computed, in post processing any subset of the elements can be analyzed. First, considering only the 2×2 covariance matrix of O_1 and O_2 , which make up the E and N terms, respectively, in the Hamiltonian Eq. (3), the diagonal elements (i.e., the conventional correlation functions) are graphed versus distance in Fig. 2(a). Here and in the following, correlation functions and eigenvalues are normalized to unity at $r = 2$, i.e., the shortest distance at which the plaquette operators do not overlap. To test convergence with the system size, results for $L = 128$ and 256 are compared. The periodic boundary conditions cause enhancements of the correlations that grow as r approaches $L/2$. Here the goal is to study relatively short distances, where these boundary effects can largely be avoided. There the two correlation functions

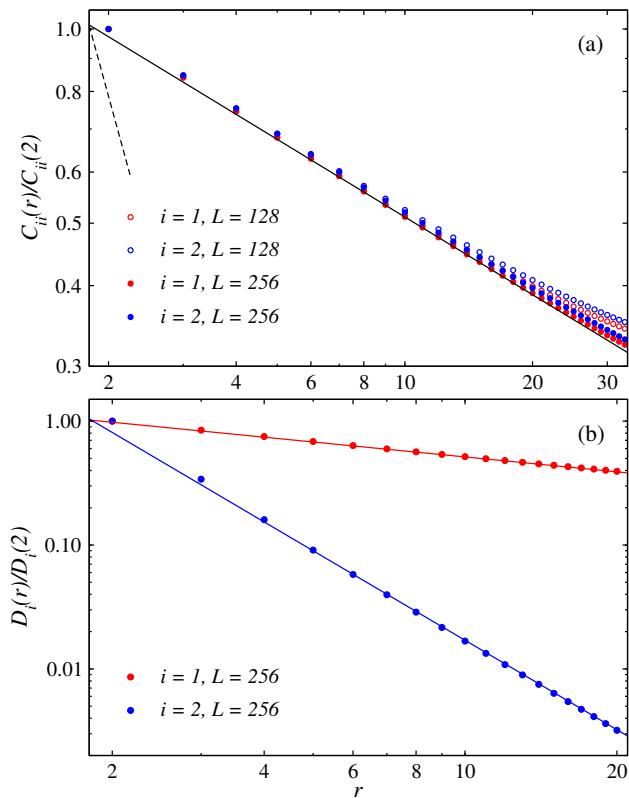


FIG. 2. (a) Normalized correlation functions of the individual operators O_1 and O_2 for $L = 128$ and 256 lattices. The solid and dashed lines show, respectively, the two power laws expected with the scaling dimensions $\Delta = 1/5$ and $6/5$ of the two relevant operators at the tricritical point. (b) Eigenvalues of the distance dependent covariance matrix of O_1 and O_2 . The lines show the same expected power laws as in (a).

are, as expected, completely dominated by the contribution from the smallest scaling dimension Δ_1 , but deviations from the leading power law are clearly visible at short distances. While there are finite-size effects left even in the limited range of r in Fig. 2, for $L = 256$ there is good agreement with the expected asymptotic exponent for $r \in [6, 20]$.

Figure 2(b) shows the eigenvalues of the 2×2 covariance matrices $C(r)$ for $L = 256$. The decay forms are indeed consistent with the two leading scaling dimensions Δ_1 and Δ_2 , though there are corrections at the shortest distances. The eigenvectors $q_i = (q_{i1}, q_{i2})$ defining $Q_i = q_{i1}O_1 + q_{i2}O_2$ are $q_1 = (q_{11}, q_{12}) = (0.731, 0.682)$ and $q_2 = (q_{21}, q_{22}) = (0.682, -0.731)$ in the range $r \in [5, 20]$, with very small changes for larger distances.

The eigenvectors mixing the two energy terms in the Hamiltonian should give the special directions in the phase diagram along which critical scaling is governed only by the corresponding correlation length exponents $\nu_1 = (2 - \Delta_1)^{-1}$ and $\nu_2 = (2 - \Delta_2)^{-1}$. The above eigenvalues were, however, computed with relative weights different from those of E and N defined in Eq. (3). The proper

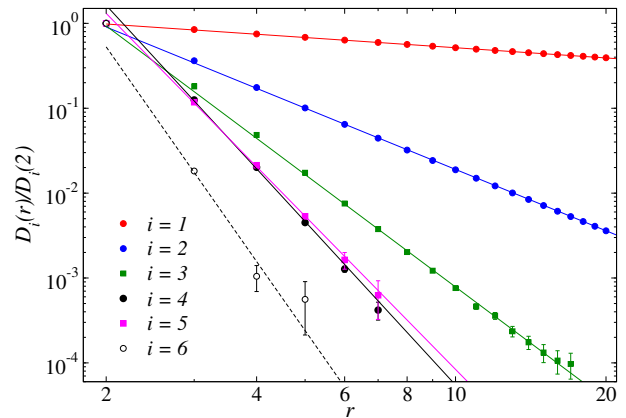


FIG. 3. (a) Normalized eigenvalues vs distance of the covariance matrix of the operators in Fig. 1. The lines drawn through the $i = 1, 2$ points show power law decays with the expected exponents $2\Delta_i = 0.4$ and $2\Delta_2 = 2.4$ of the relevant operators. The other lines show the exponents expected with the four smallest irrelevant dimensions; $2\Delta_3 = 4.4$, $2\Delta_4 = 6.4$, $2\Delta_5 = 6$, and $2\Delta_6 = 8.4$. The amplitudes at $r = 2$ before normalizing are (including statistically significant digits) 6.25×10^{-1} , 1.28×10^{-2} , 1.60×10^{-4} , 2.35×10^{-5} , 1.80×10^{-6} , and 2.4×10^{-7} , for $i = 1, \dots, 6$.

weighting of the two operators is obtained with $2O_1$ and O_2 , which gives the eigenvectors $q_1 = (0.906, 0.423)$ and $q_2 = (0.423, -0.906)$ (i.e., the ratio of the coefficients trivially change by a factor of 2). With the Ising interaction strength set to unity in Eq. (3), one of these vectors should define the tangential direction at the tricritical point of the phase boundary expressed as $\mu_c = -(\beta\lambda)_c$ versus β , where $\beta \equiv T^{-1}$. Examining the phase boundary λ_c versus T in Fig. 1 of Ref. [13] (which uses slightly different notation), a derivative $d\lambda_c/dT \approx -0.28$ at the tricritical point can be estimated. This translates to $d\mu_c/d\beta \approx -2.17$, which should equal the ratio q_{i2}/q_{i1} for one of the eigenvectors ($i = 1$ or $i = 2$) of the covariance matrix. Indeed, the derivative closely matches q_2 (corresponding to $\Delta_2 = 6/5$), with $q_{22}/q_{21} \approx -0.906/0.423 \approx -2.14$. This agreement within less than 2% is as good as could possibly be expected, given the uncertainty of the tangent estimated from the phase diagram in Ref. [13].

Moving on to the full 6×6 covariance matrix, Fig. 3 shows $L = 256$ results for $D_i(r)$ up to $r = 20$, where the boundary effects are small. Remarkably, all six lowest scaling dimensions ($\Delta_i = 0.2, 1.2, 2.2, 3, 3.2$, and 4.2) are correctly reflected in the observed power-law decays, though in the case $i = 6$ ($\Delta_6 = 4.2$ expected) the statistical uncertainty is large. For the other cases, fitting to a single power law in a window of r where this is possible gives (with one standard error) $\Delta_1 = 0.199 \pm 0.001$ ($r \in [6, 20]$), $\Delta_2 = 1.199 \pm 0.001$ ($r \in [6, 20]$), $\Delta_3 = 2.26 \pm 0.03$ ($r \in [6, 17]$), $\Delta_4 = 3.19 \pm 0.02$ ($r \in [3, 7]$), and $\Delta_5 = 2.99 \pm 0.04$ ($r \in [3, 7]$). Note that the eigenvalues $D_i(r)$ are ordered according to their $r = 2$ pre-

normalization values (listed in the caption of Fig. 3) and Δ_i then do not necessarily increase with i . No crossings of $D_i(r)$ versus r for different i are observed here.

It would be impossible to extract all of these scaling dimensions from a conventional correlation function. At most the two smallest dimensions can be extracted by fitting power laws, at worse fidelity than achieved here. Even though the overall amplitudes before normalization decay very rapidly with i , the statistical precision is maintained at a level far below the statistical errors of the original data. This statistical advantage likely reflects correlated fluctuations of the elements of the covariance matrix (higher-order covariance).

There are still corrections to the asymptotic power laws in Fig. 3 which should arise from the fact that the model itself is not exactly at the tricritical Ising fixed point, because of inevitably present irrelevant operators. The results here demonstrate very clearly that these corrections do not produce additional independent power laws but induce corrections to each individual CFT power law—effectively to the individual scaling dimensions—that decay away with increasing length scale (here r). This behavior is analogous to what is observed in 2+1 dimensional numerical CFT realizations on tiled (polyhedron) [16, 17] and fuzzy [2, 3, 18] spheres, where the dimensions evolve with the system size.

In conventional data fitting, $\propto r^{-2\Delta_i+d-\Delta_j}$ corrections to $r^{-2\Delta_i}$ correlations from irrelevant fields ($\Delta_j > d$) and contributions from multiple unperturbed CFT power laws cannot be separated. In the covariance method, the CFT power laws are disentangled and fitting only requires one relevant scaling dimension for each i , possibly with irrelevant corrections. In the BC model the corrections are negligible already at moderate values of r .

The eigenvectors corresponding to the three smallest scaling dimensions in Fig. 3 are

$$q_1 \approx \begin{pmatrix} 0.436 \\ 0.407 \\ 0.444 \\ 0.403 \\ -0.379 \\ -0.375 \end{pmatrix} \quad q_2 \approx \begin{pmatrix} 0.179 \\ -0.138 \\ 0.328 \\ 0.549 \\ 0.448 \\ 0.583 \end{pmatrix} \quad q_3 \approx \begin{pmatrix} 0.253 \\ 0.025 \\ 0.619 \\ -0.715 \\ 0.123 \\ 0.162 \end{pmatrix},$$

where the elements from top to bottom are the coefficients of O_1, \dots, O_6 in Fig. 1(b). Here q_1 and q_2 change very little with r , while q_3 is statistically noisy for $r > 10$ but does not change appreciably between $r = 4$ and $r = 10$. The above results are all for $r = 10$. Note that the coefficients of all individual operators O_i are typically of the same order, showing that none of them completely dominates the overlaps with the CFT operators.

Unlike the $n = 2$ case discussed earlier, for $n = 6$ the relationship between the eigenvectors and the special directions in the two-dimensional phase diagram is nontrivial, given that the original operators O_i are not orthogonal, and an analysis of the full six-dimensional

space would be necessary. It is interesting to note, however, that the eigenvector q_1 has almost exactly the same ratio of coefficients, $q_{11}/q_{12} \approx 1.07$ as in the 2×2 case, which is not true for the second eigenvector, where now $q_{22}/q_{21} \approx -0.78$ (instead of -1.07 in the 2×2 case).

Discussion.—The results obtained here demonstrate that the covariance method is capable of resolving multiple scaling dimensions in remarkable detail, far beyond what is possible by fitting conventional correlation functions to a sum of power laws. The ability to also extract the eigenfunctions corresponding to relevant orthogonal operators is also an appealing feature, with many potential applications to multicriticality, e.g., deconfined quantum-critical points [19–22], and in studies of liquid-gas transitions. The method is easy to implement with any MC or quantum MC simulation and should be applicable also with other numerical approaches.

Here the limit $r \ll L$ was targeted to avoid boundary effects. Alternatively, the L dependence of the eigenvalues at $r = aL$ with fixed a can be analyzed, e.g., $r = L/2$. In quantum systems, it will also be useful to study the covariance matrix as a function of imaginary time τ . A method in spirit similar to the one used here to separate different power laws was years ago employed to study exponentially decaying τ correlations in a system with discrete energy levels [23]. For a finite quantum system at $T = 0$, the discreteness of the level spectrum implies exponential decays asymptotically for $\tau \rightarrow \infty$. However, for a sufficiently large critical system described by a CFT, the τ dependence for τ up to order L should be a sum of power laws governed by scaling dimensions, like the real-space correlations analyzed here (and more generally space and time correlations are related by a dynamic exponent [24]). It would be interesting to study the crossover from power laws to exponentials in the eigenvalues and -vectors of the covariance matrix in quantum MC simulations [25] within the fuzzy sphere approach [2, 3].

The closest MC based competitors to the covariance scheme would likely be MC renormalization-group methods, which have a long history [26], including in the context of the same BC model studied here [6, 7]. Recently this approach has been further developed by adapting neural networks (machine learning) to construct lattice realizations of continuum field operators [27]. Training a neural network using MC samples, some of these methods make use of covariance and principal value analysis to optimize a set of orthogonal operators [28–31]. The general setup is, however, very different from, and much more complicated than, the covariance method demonstrated here, where the initial operators can be essentially arbitrary and their linear combinations found by diagonalization are the optimized operators. Results from machine learning methods so far also do not appear to be competitive with what was achieved in the test case here with only modest computational resources (about

10^4 CPU hours spent on the results in Fig. 3). It would certainly be interesting to compare the performance of the methods for some challenging model.

Acknowledgments.—The author would like to thank Dong-Hee Kim and Masaki Oshikawa for valuable discussions and Emilie Huffman for comments and for pointing out Ref. 23. This research was supported by the Simons Foundation under Grant No. 511064 and in part by Grant No. NSF PHY-2309135 to the Kavli Institute for Theoretical Physics (KITP). The numerical calculations were carried out on the Shared Computing Cluster managed by Boston University’s Research Computing Services.

* sandvik@bu.edu

- [1] D. Poland, S. Rychkov, and A. Vichi, *The Conformal Bootstrap: Theory, Numerical Techniques, and Applications*, *Rev. Mod. Phys.* **91**, 15002 (2019).
- [2] W. Zhu, C. Han, E. Huffman, J. S. Hofmann, and Y.-C. He, *Uncovering Conformal Symmetry in the 3D Ising Transition: State-Operator Correspondence from a Quantum Fuzzy Sphere Regularization*, *Phys. Rev. X* **13**, 021009 (2023).
- [3] Z. Zhou, L. Hu, W. Zhu, Y.-C. He, *The SO(5) Deconfined Phase Transition under the Fuzzy Sphere Microscope: Approximate Conformal Symmetry, Pseudo-Criticality, and Operator Spectrum*, arXiv:2306.16435.
- [4] I. Affleck and F. D. M. Haldane, *Critical theory of quantum spin chains*, *Phys. Rev. B* **36**, 5291 (1987).
- [5] P. Di Francesco, P. Mathieu, and D. Sénéchal, *Conformal Field Theory, Vol. 1* (Springer-Verlag, New York 1997).
- [6] D. P. Landau and R. H. Swendsen, *Tricritical Universality in Two Dimensions*, *Phys. Rev. Lett.* **46**, 1437 (1981).
- [7] D. P. Landau and R. H. Swendsen, *Monte Carlo renormalization-group study of tricritical behavior in two dimensions*, *Phys. Rev. B* **33**, 7700 (1986).
- [8] P. D. Beale, *Finite-size scaling study of the two-dimensional Blume-Capel model*, *Phys. Rev. B* **33**, 1717 (1986).
- [9] N. B. Wilding and P. Nielaba, *Tricritical universality in a two-dimensional spin fluid*, *Phys. Rev. E* **53**, 926 (1996).
- [10] Y. Deng and H. Blöte, *Edge phase transitions of the tricritical Potts model in two dimensions*, *Phys. Rev. E* **71**, 026109 (2005).
- [11] C. J. Silva, A. A. Caparica, and J. A. Plascak, *Wang-Landau Monte Carlo simulation of the Blume-Capel model*, *Phys. Rev. E* **73**, 036702 (2006).
- [12] J. A. Plascak and P. H. L. Martins, *Probability distribution function of the order parameter: Mixing fields and universality*, *Comput. Phys. Commun.* **184**, 259 (2013).
- [13] W. Kwak, J. Jeong, J. Lee, and D.-H. Kim, *First-order phase transition and tricritical scaling behavior of the Blume-Capel model: A Wang-Landau sampling approach*, *Phys. Rev. E* **92**, 022134 (2015).
- [14] B. Nienhuis, *Analytical calculation of two leading exponents of the dilute Potts model*, *J. Phys. A: Math. Gen.* **15** 199 (1982).
- [15] R. H. Swendsen and J.-S. Wang, *Nonuniversal critical dynamics in Monte Carlo simulations*, *Phys. Rev. Lett.* **58**, 86 (1987).
- [16] B.-X. Lao and S. Rychkov, *3D Ising CFT and Exact Diagonalization on Icosahedron: The Power of Conformal Perturbation Theory*, *SciPost Phys.* **15**, 243 (2023).
- [17] V. Ayyar, R. C. Brower, G. T. Fleming, A.-M. E. Glück, E. K. Owen, T. G. Raben, and C.-I. Tan, *The Operator Product Expansion for Radial Lattice Quantization of 3D ϕ^4 Theory*, arXiv:2311.01100.
- [18] B.-B. Chen, X. Zhang, and Z. Y. Meng, *Emergent Conformal Symmetry at the Multicritical Point of (2+1)D SO(5) Model with Wess-Zumino-Witten Term on Sphere*, arXiv:2405.04470.
- [19] B. Zhao, J. Takahashi, and A. W. Sandvik, *Multicritical Deconfined Quantum Criticality and Lifshitz Point of a Helical Valence-Bond Phase*, *Phys. Rev. Lett.* **125**, 257204 (2020).
- [20] B.-B. Chen, X. Zhang, Y. Wang, K. Sun, and Z. Y. Meng, *Phases of (2+1)D SO(5) non-linear sigma model with a topological term on a sphere: multicritical point and disorder phase*, arXiv:2307.05307.
- [21] S. M. Chester and N. Su, *Bootstrapping Deconfined Quantum Tricriticality*, *Phys. Rev. Lett.* **132**, 111601 (2024).
- [22] J. Takahashi, H. Shao, B. Zhao, W. Guo, and A. W. Sandvik, *SO(5) multicriticality in two-dimensional quantum magnets*, arXiv:2405.06607.
- [23] M. Lüscher and U. Wolff, *How to calculate the elastic scattering matrix in two-dimensional quantum field theories by numerical simulation*, *Nucl. Phys. B* **339**, 222 (1990).
- [24] M. P. A. Fisher, P. B. Weichman, G. Grinstein, and D. S. Fisher, *Boson localization and the superfluid-insulator transition*, *Phys. Rev. B* **40**, 546 (1989).
- [25] J. S. Hofmann, F. Goth, W. Zhu, Y.-C. He, and E. Huffman, *Quantum Monte Carlo Simulation of the 3D Ising Transition on the Fuzzy Sphere*, arXiv:2310.19880.
- [26] R. H. Swendsen, in *Real Space Renormalization*, edited by T. Burkhardt and J. M. J. van Leeuwen (Springer-Verlag, Berlin, 1982).
- [27] M. Koch-Janusz and Z. Ringel, *Mutual information, neural networks and the renormalization group*, *Nature Phys.* **14**, 578 (2018).
- [28] A. Gordon, A. Banerjee, M. Koch-Janusz, and Z. Ringel, *Relevance in the Renormalization Group and in Information Theory*, *Phys. Rev. Lett.* **126**, 240601 (2021).
- [29] D. E. Gökmenn, Z. Ringel, S. D. Huber, and M. Koch-Janusz, *Statistical Physics through the Lens of Real-Space Mutual Information*, *Phys. Rev. Lett.* **127**, 240603 (2021).
- [30] D. E. Gökmenn, Z. Ringel, S. D. Huber, and M. Koch-Janusz, *Symmetries and phase diagrams with real-space mutual information neural estimation*, *Phys. Rev. E* **104**, 064106 (2021).
- [31] L. Oppenheim, M. Koch-Janusz, S. Gazit, and Z. Ringel, *Machine Learning the Operator Content of the Critical Self-Dual Ising-Higgs Gauge Model*, arXiv:2311.17994.